Research Article | Vol. 25, No. 8 | 17 Apr 2017 | OPTICS EXPRESS 9225

Optics EXPRESS

Specific distribution of the light captured by silver nanowire

YINGFENG LI,[1] YOUNAN LUO,[1] WENJIAN LIU,[1] MENGQI CUI,[1] JERRY KUMAR,[1] BING JIANG,[1] LIHUA CHU,[1] AND MEICHENG LI[1,2,*]

[1]*State Key Laboratory of Alternate Electrical Power System with Renewable Energy Sources, North China Electric Power University, Beijing 102206, China*
[2]*Chongqing Materials Research Institute, Chongqing 400707, China*
**mcli@ncepu.edu.cn*

Abstract: The silver nanowire (AgNW) has excellent light capture ability, showing great prospects in many fields. Based on discrete dipole approximation simulations, it is found that the captured light can be subdivided into three parts: the near-field light occupies ~27.3%, mainly confined around the nanowire with a distance <20nm; the far-field part occupies ~59.6%, showing a dramatic conical distribution; and ~13.1% is ohmically absorbed. These insights are helpful to estimate the limited performance of AgNW-based device utilizing each subdivision, and locate the functional zone. Besides, we found that the light capture efficiency of AgNW can be easily controlled as it increases linearly with nanowire length.

OCIS codes: (290.0290) Scattering; (290.2200) Extinction; (290.5838) Scattering, in-field; (160.4236) Nanomaterials; (220.0220) Optical design and fabrication.

References and links

1. V. Laprévote, A. Oliva, C. Delerue, P. Thomas, and M. Boucart, "Patients with schizophrenia are biased toward low spatial frequency to decode facial expression at a glance," Neuropsychologia **48**(14), 4164–4168 (2010).
2. H. Chen, L. Shao, Q. Li, and J. Wang, "Gold nanorods and their plasmonic properties," Chem. Soc. Rev. **42**(7), 2679–2724 (2013).
3. H. Dong, Z. Wu, F. Lu, Y. Gao, A. El-Shafei, B. Jiao, S. Ning, and X. Hou, "Optics–electrics highways: Plasmonic silver nanowires@ TiO 2 core–shell nanocomposites for enhanced dye-sensitized solar cells performance," Nano Energy **10**, 181–191 (2014).
4. J. P. Kottmann, O. J. Martin, D. R. Smith, and S. Schultz, "Plasmon resonances of silver nanowires with a nonregular cross section," Phys. Rev. B **64**(23), 235402 (2001).
5. Q. N. Luu, J. M. Doorn, M. T. Berry, C. Jiang, C. Lin, and P. S. May, "Preparation and optical properties of silver nanowires and silver-nanowire thin films," J. Colloid Interface Sci. **356**(1), 151–158 (2011).
6. C. J. Murphy and N. R. Jana, "Controlling the aspect ratio of inorganic nanorods and nanowires," Adv. Mater. **14**(1), 80–82 (2002).
7. K. Ni, L. Chen, and G. Lu, "Synthesis of silver nanowires with different aspect ratios as alcohol-tolerant catalysts for oxygen electroreduction," Electrochem. Commun. **10**(7), 1027–1030 (2008).
8. X. Zhang, Y. L. Chen, R.-S. Liu, and D. P. Tsai, "Plasmonic photocatalysis," Rep. Prog. Phys. **76**(4), 046401 (2013).
9. X. Xiong, C. L. Zou, X. F. Ren, A. P. Liu, Y. X. Ye, F. W. Sun, and G. C. Guo, "Silver nanowires for photonics applications," Laser Photonics Rev. **7**(6), 901–919 (2013).
10. C. Li, M. Bescond, and M. Lannoo, "Influence of the interface-induced electron self-energy on the subthreshold characteristics of silicon gate-all-around nanowire transistors," Appl. Phys. Lett. **97**(25), 252109 (2010).
11. A. L. Pyayt, B. Wiley, Y. Xia, A. Chen, and L. Dalton, "Integration of photonic and silver nanowire plasmonic waveguides," Nat. Nanotechnol. **3**(11), 660–665 (2008).
12. C. Delerue, G. Allan, J. Pijpers, and M. Bonn, "Carrier multiplication in bulk and nanocrystalline semiconductors: Mechanism, efficiency, and interest for solar cells," Phys. Rev. B **81**(12), 125306 (2010).
13. C. Delerue, V. Laprévote, K. Verfaillie, and M. Boucart, "Gaze control during face exploration in schizophrenia," Neurosci. Lett. **482**(3), 245–249 (2010).
14. Y. Sun and Y. Xia, "Shape-controlled synthesis of gold and silver nanoparticles," Science **298**(5601), 2176–2179 (2002).
15. Y. Cui, I. Y. Phang, R. S. Hegde, Y. H. Lee, and X. Y. Ling, "Plasmonic silver nanowire structures for two-dimensional multiple-digit molecular data storage application," ACS Photonics **1**(7), 631–637 (2014).
16. H. Ditlbacher, A. Hohenau, D. Wagner, U. Kreibig, M. Rogers, F. Hofer, F. R. Aussenegg, and J. R. Krenn, "Silver nanowires as surface plasmon resonators," Phys. Rev. Lett. **95**(25), 257403 (2005).

#283028 https://doi.org/10.1364/OE.25.009225
Journal © 2017 Received 20 Feb 2017; revised 31 Mar 2017; accepted 31 Mar 2017; published 12 Apr 2017

Optics EXPRESS

17. M. A. El-Sayed, "Some interesting properties of metals confined in time and nanometer space of different shapes," Acc. Chem. Res. **34**(4), 257–264 (2001).
18. W. Wang, Q. Yang, F. Fan, H. Xu, and Z. L. Wang, "Light propagation in curved silver nanowire plasmonic waveguides," Nano Lett. **11**(4), 1603–1608 (2011).
19. Y. Li, M. Li, R. Li, P. Fu, L. Chu, and D. Song, "Method to determine the optimal silicon nanowire length for photovoltaic devices," Appl. Phys. Lett. **106**(9), 091908 (2015).
20. A. B. Evlyukhin, C. Reinhardt, and B. N. Chichkov, "Multipole light scattering by nonspherical nanoparticles in the discrete dipole approximation," Phys. Rev. B **84**(23), 235429 (2011).
21. S. H. Simpson and S. Hanna, "Application of the discrete dipole approximation to optical trapping calculations of inhomogeneous and anisotropic particles," Opt. Express **19**(17), 16526–16541 (2011).
22. B. T. Draine and P. J. Flatau, "User guide for the discrete dipole approximation code DDSCAT 7.3," https://arxiv.org/abs/1305.6497 (2013).
23. B. T. Draine and P. J. Flatau, "Discrete-dipole approximation for scattering calculations," J. Opt. Soc. Am. A **11**(4), 1491–1499 (1994).
24. P. J. Flatau and B. T. Draine, "Fast near field calculations in the discrete dipole approximation for regular rectilinear grids," Opt. Express **20**(2), 1247–1252 (2012).
25. Y. Li, L. Yue, Y. Luo, W. Liu, and M. Li, "Light harvesting of silicon nanostructure for solar cells application," Opt. Express **24**(14), A1075–A1082 (2016).
26. Y. Li, M. Li, D. Song, H. Liu, B. Jiang, F. Bai, and L. Chu, "Broadband light-concentration with near-surface distribution by silver capped silicon nanowire for high-performance solar cells," Nano Energy **11**, 756–764 (2015).
27. Y. Li, M. Li, P. Fu, R. Li, D. Song, C. Shen, and Y. Zhao, "A comparison of light-harvesting performance of silicon nanocones and nanowires for radial-junction solar cells," Sci. Rep. **5**, 11532 (2015).
28. O. S. Wolfbeis, M. Schäferling, and A. Dürkop, "Reversible optical sensor membrane for hydrogen peroxide using an immobilized fluorescent probe, and its application to a glucose biosensor," Mikrochim. Acta **143**, 221–227 (2003).
29. C.-S. Chu and Y.-L. Lo, "Ratiometric fiber-optic oxygen sensors based on sol–gel matrix doped with metalloporphyrin and 7-amino-4-trifluoromethyl coumarin," Sens. Actuators B Chem. **134**(2), 711–717 (2008).
30. Z. Guo, J. Liu, Y. Jia, X. Chen, F. Meng, M. Li, and J. Liu, "Template synthesis, organic gas-sensing and optical properties of hollow and porous In2O3 nanospheres," Nanotechnology **19**(34), 345704 (2008).
31. D. W. Lynch and W. Hunter, "Comments on the optical constants of metals and an introduction to the data for several metals," in *Handbook of Optical Constants of Solids* (Academic Press, 1985).

1. Introduction

The silver nanowire (AgNW) shows excellent light capture ability [1–4]: the extinction cross section of AgNW can even reach micron size; and the fabrication technology of it is advancing to a level that the diameter, length and surface qualities can be well controlled [5,6].Therefore, it has been tentatively applied in many fields like photon catalytic [7,8], optical sensors [9], biological/chemical sensors [10], photon waveguide [11], surface enhanced Raman scattering [12,13], and photovoltaics [14]. For instance, by integrating multiple AgNWs together, Pyayt et al [11] have realized to confine and guide light on a chip based on controlling the light coupling degree between two adjacent nanowires. Cui et al [15] have achieved a 2-dimensional 7-digit optical molecular data storage system using homogeneous plasmonic AgNW architecture.

In specific applications, not all of the light captured by AgNW is useful but only special parts are of great significance. For example, when using AgNW in catalytic [7], sensor [9,10], wave guide [11] and surface enhanced Raman scattering [12], the localized near-filed light, whose intensity and distribution mainly determines the device performance, is especially important. While, if AgNW is used in photovoltaics for light-trapping [14] or used as surface plasmon resonators [2], the amount and distribution features of the far-filed light become more important. Except for above parts, the light being ohmically adsorbed within the AgNW is even harmful as it will be transformed to heat thus reduce the device performance and lifetime. Therefore, the proportions of the near-field light, the far-field scattering light, and the ohmically adsorbed part in the total captured light and their distributions are investigated here in details.

Due to the unique one dimensional character of AgNW, length is also an important parameter for its practical applications in many fields [9,11,15,16]. It dramatically affects the detecting signal intensity in AgNW-based sensors, as it determines the amount of matters

Optics EXPRESS

(need to be detected) that can be attached on the nanowire; and it limits the transportation distance of light in plasmonic waveguide. Till now, only few studies have come down to the influence of length on the optical properties of AgNW. El-Sayed et al [17] have discovered the red-shift of the longitudinal mode of AgNW with increased aspect ratio. Wang et al [18] have reported the dramatic light loss when propagating through bended AgNW. However, there is still no reports on the common length dependencies for the light capture ability of AgNW, which is significant and necessary.

DDSCAT 7.3 is a software package can give reliable numerical solutions on the electromagnetic scattering of nanostructures with arbitrary shape and material [19–24], based on discrete dipole approximation (DDA). Its accuracy and reliability have been well verified in our previous works [25–27]. In this work, at first, we investigated the specific distribution of the light captured by AgNW; then we investigated the length dependency of the light-capture ability of AgNW, using DDA method. These pieces of information can provide fundamental directions for the design of high-performance photonic devices built on AgNW.

2. Model and method

AgNW is modeled as a circular cylinder as shown in Fig. 1(a). The diameter of AgNW is fixed to 80nm, which corresponds to a resonance wavelength (RW) ~400nm, required in many gas sensors [28–30]; and its length is fixed to 1μm in investigating the specific distribution of the light captured by AgNW, and varies from 1 to 10μm in investigating the length dependent light-capture ability. Since the samples of AgNW are large enough, the quantum confinement effect can be neglected and thus the bulk values of the complex index of refraction for silver are used [31], as given in Fig. 1(b).

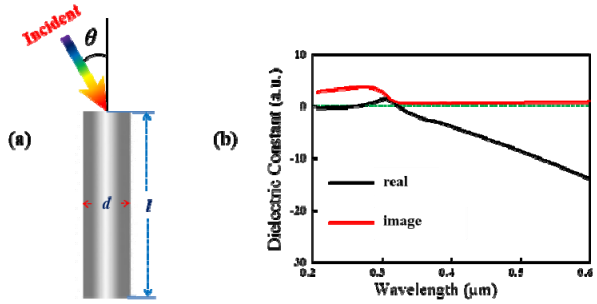

Fig. 1. (a) Schematic of AgNW; and (b) the complex index of refraction for silver.

The optical properties of AgNW are simulated using the software package DDSCAT 7.3. In the framework of DDA, AgNW is treated as an array of point dipoles located on cubic lattices. The optical response of AgNW is obtained by solving the electromagnetic scattering problem of the incident light interacting with this point dipoles array, using iterative method. The accuracy of the simulations is mainly determined by the size of the point dipoles, whose side length has been set as 3.3nm according to carefully tests [26]. The other parameter affecting the simulation accuracy is the error tolerance between two adjacent iterative steps. In our simulations, it is set to be 1.0×10^{-5}, which corresponds to high accuracy [22].

In DDSCAT 7.3, the light-capture ability of AgNW is characterized by the extinction, scattering and absorption efficiencies, which are defined as $Q_{ext} = C_{ext}/\pi r^2$, $Q_{sca} = C_{sca}/\pi r^2$ and $Q_{abs} = C_{abs}/\pi r^2$, respectively. r is the real geometric radius of AgNW; C_{ext}, C_{sca}, C_{abs} and πr^2 refer to the extinction, scattering, absorption and geometric cross section of AgNW. Therefore, Q_{ext} reflects the wavelength selective light-concentration ability; Q_{sca} stands for the light-scattering ability; and Q_{abs} denotes the intrinsic light absorption, which is generally defined as the ohmic loss, in AgNW.

Optics EXPRESS

3. Results and discussion

3.1 Influences of the incident angle

The incident angle, which is denoted by θ as shown in Fig. 1(a), is an important parameter affecting the optical properties of AgNW. Therefore, at the beginning, we investigate its influences on the light-capture ability of AgNW (wavelength selective extinction cross section), based on a sample with length 1μm and diameter 80nm.

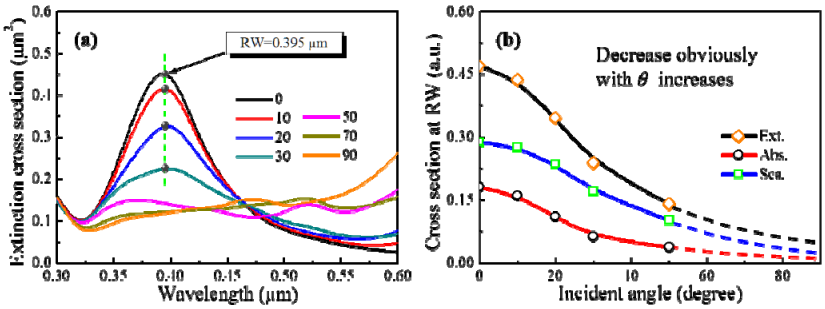

Fig. 2. (a) Influence of incident angle on the extinction cross-section of AgNW with 80nm diameter and 1μm length; (b) relationship between the cross-section at RW and θ, where dashed lines are used to denote corresponding values at wavelength 0.395μm when θ is greater than 50° as there is no obvious RW in these cases.

Relationships between RW, extinction cross section of AgNW and θ are presented in Fig. 2(a). It can be observed that RW depends weakly on θ when θ ranges from 0° to 30°: RW is about 0.395μm. This indicates, in this range of incident angles, AgNW (or structure of great aspect ratio) supports a strong plasmon dipole mode, whose RW is mainly determined by the diameter thus shift slightly with θ. If θ is greater than 50°, there is no obvious RW on the curves; and the extinction cross sections over the whole waveband, about 0.1μm^2, are just a little greater than the nanowire's geometric cross section, 0.08μm^2. This is because as θ increases, the projected size of AgNW on the polarization direction of the incident light increases (diameter/cosθ). As a consequence, the retardation effects become significant, and therefore higher order multiple modes (starting with the quadrupole mode) appear. Such modes have wide resonance wavebands; therefore, they overlap each other and such overlapping tends to obscure some of the peaks. As a conclusion, it is better to keep the incident angle to be less than 30° in real applications.

Different from RW, the extinction cross section C_{ext} varies (decreases) dramatically with θ, which can be more clearly reflected in Fig. 2(b), by the variation tendency of the maximum C_{ext} values (at RW) in Fig. 2(a) with different θ. Therein, corresponding variation curves of C_{abs} and C_{sca} are also provided. As mentioned above, C_{ext}, C_{abs} and C_{sca} denotes the light concentration, absorption and scattering ability of AgNW respectively, thus they are important indexes in many application fields. Notably, all of C_{ext}, C_{abs} and C_{sca} at RW show the largest values when θ = 0°, and decrease dramatically with increases in θ. Therefore, incidence paralleling to the nanowire should be the best choice to capture as much light in practical applications; and allowing this, θ has been fixed to 0° in following investigations.

3.2 The specific distribution of the captured light

As mentioned above, not all of the light captured by AgNW is useful but only special parts are of great significance in specific applications. According to the distance from the AgNW, the light out the nanowire can be separated into localized near-field light and far-field light. At first, the distribution of the near-field part is investigated. The near-field distribution of the electric field, whose square is equal to the light intensity, in and around the nanowire is given in Fig. 3(a). It can be seen that, the maximum near-field light intensity (denoted by the red

Optics EXPRESS

color) can reach 40 multiples of the incident light ($|E|^2/|E_0|^2$, $|E|/|E_0| \approx 6$ from the legend); and the range owning strong near-field light only distribute out the nanowire within distance about 20nm (from In1). To describe such distribution quantitatively, we divided the cross section into 100 annuluses with identical Δr (the inset in In2), integrated the square of the field intensities over every annulus, and got the distribution of these integrations in In2. It is found that 20nm just corresponds to the distance where the light intensity reduces to e^{-1} from the surface of AgNW; and over 65% of the near-field light (the amount of light in a 240nm × 240nm square) localizes within this distance. Such strong intensity and the near-surface distribution feature indicate that, when using AgNW as the building block of sensors or photo detectors, the functional groups are better to be mounted in near-surface areas and the matters need to be detected must can enter into these areas. The most effective inter-guide light coupling also should occur within a distance of 20nm.

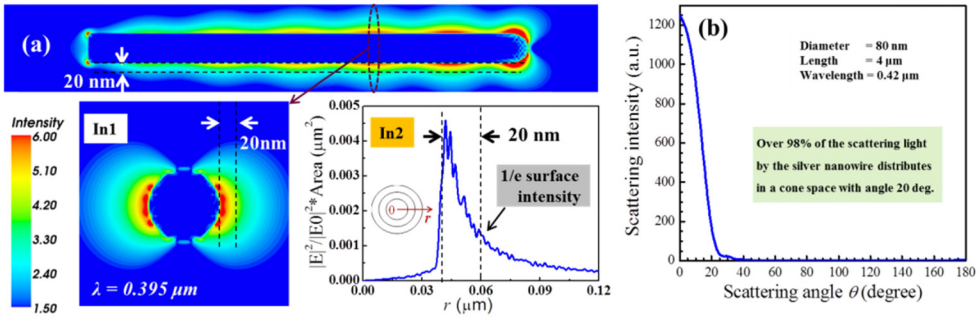

Fig. 3. (a) Electric field distributions in and around AgNW, under incident light with λ = 0.395μm. In1: cross section; In2: radial distribution of the light intensity ($|E|^2/|E_0|^2 * area$), which is calculated by dividing the cross section into 100 annuluses and integrating over each of them. (b) Angle distribution of the scattering light.

It can be also estimated that the proportion of the near-field light occupies about 27.3% of the total captured light. This value is calculated through first converting the integrated amount of near-field light in In2, 0.31 a.u., to a time-averaged value $0.31 \times 4/\pi^2$ and then dividing it by the extinction cross section of the nanowire, 0.46, as shown in Fig. 2(b): $0.31 \times 4/\pi^2/0.46 \approx 27.3\%$. This high proportion confirms the importance of the near-field light around AgNW from a quantitative view of point. Besides, from Fig. 3(a) we can also see that both the intensity and range of the near-field light damps dramatically along the propagation of the incident light, which indicate that the functional zone of AgNW based devices is better to locate near the top of the nanowire.

Then, the distribution of the far-field light is studied. The far-field scattering light can occupy about 59.6% of the light being captured (calculated through dividing the scattering cross section by the extinction using the data in Fig. 2(b)), therefore, taking full advantage of this part of light is important. The distribution of the far-field scattering light is given in Fig. 3(c), which shows largely angle dependent: over 98% of it distributes in a cone space around the nanowire with narrow angle range, θ<20°. The large proportion and direction output of the far-field light means that AgNW can be used as light trapping structure in photovoltaic devices. Cooperating with its wave-guide function, such directional scattering feature also indicates AgNW is able to be used as an effective nanoscale on-chip light source or on-chip light transceiver.

To take heed, in above case, except for the near-field light (27.3%) and the part being scattered (59.6%), there is still about 13.1% of the total captured light will be absorbed by the nanowire itself (this value is not accuracy because that the near-field light contains some contribution from the scattering light, but the order of magnitude should be right). As mentioned above, this part of light will be transformed to thermo energy, thus is harmful for

Optics EXPRESS

the device performance. Therefore, in the design of AgNW based devices, schemes to avoid or reduce the influences of ohmic loss must be taken into account.

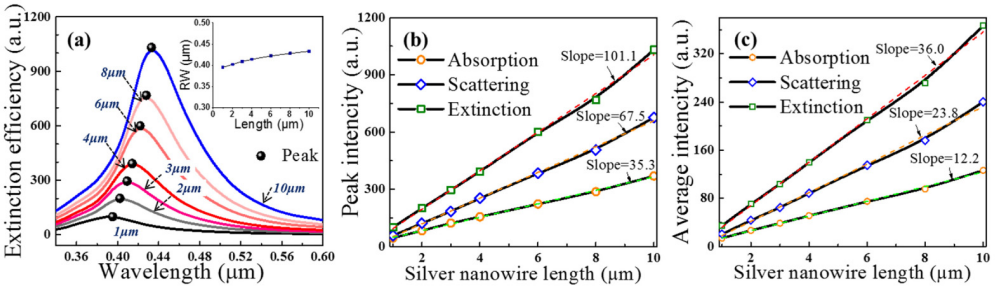

Fig. 4. (a) Extinction efficiencies of AgNW with lengths from 1 to 10μm, with inset about the variation of RW with length; (b) Relationship of the maximum extinction, scattering and absorption efficiencies at RW to the lengths; (c) Relationship of average extinction, scattering and absorption efficiencies in waveband 0.2-0.6μm to the lengths.

3.3 The length dependency for the light capture ability of AgNW

Length is key parameter of AgNW during its practical applications in many fields [9,11,15,16]. Thus, it is quite necessary to reveal the relationships between the light-capture ability of AgNW and its length. The extinction efficiency curves of AgNWs with various lengths from 1 to 10μm and fixed diameter of 80nm are presented in Fig. 4(a). It can be seen that RW increases with the length, but with quite small extent: it increases first rapidly and then slowly from 0.395μm to a stable value about 0.43μm, as shown in the inset. This implies RW of AgNW is mainly determined by the diameter, but can be also weakly influenced by the length especially when it is short.

Different from RW, the light capture ability of AgNW depends dramatically on the length as shown in Fig. 4(a). To go further, we distinguished the light capture ability into three aspects: light-concentration, -scattering and -absorption abilities, which can be characterized by the extinction, scattering and absorption efficiencies mentioned above; and investigated their length dependencies respectively. Figure 4(b) gives the variation tendencies of the extinction, scattering and absorption efficiencies at RW with the length of AgNW. It can be seen that all of the extinction, scattering and absorption efficiencies increase in a linear fashion with the length of AgNW. This can be well explained by the Mie theory, based on which the extinction efficiency Q_{ext} for a spherical metallic particle can be deduced to be about 12 $V/(\varepsilon'' \lambda)$, where V is the volume of the sphere, λ is the vacuum wavelength of light and ε'' is the imaginary part of dielectric constant. According to Fig. 1(b) the item $\varepsilon'' \lambda$ will have a constant minimum, therefore the maximum extinction efficiency, Q_{ext}^{max}, should be proportional to the volume. For AgNW, $V = \pi r^2 \times l$, where r and l is the radius and the length of AgNW respectively; r is fixed, therefore the maximum extinction efficiency, Q_{ext}^{max}, should increase linearly with the length.

In Fig. 4(c) we show the variation tendencies of the full-spectrum (0.2-0.6μm) averaged extinction, scattering and absorption efficiencies of AgNW with its length. Surprisingly, they also increase in a linear fashion with the length of AgNW. These indicate the light capture ability of AgNW is linear to length in the whole waveband. Such simple linear dependency indicates that the light capture ability of AgNW can be easily controlled by changing the nanowire length. The slopes for the fitted dash lines in Fig. 4(b) and 4(c) are related to the diameter of AgNW.

Optics EXPRESS

4. Conclusion

In summary, based on the DDA simulations, specific subdivision for the light captured by AgNW were provided. It is found that the near-field light occupied a great proportion of the light being captured (27.3%), with dramatic near surface distribution. This confirms the good quality of the near-field light and implies where the functional zones should be located at during the utilization of AgNW. The far-field scattering light occupies about 59.6%, with 98% of it distributes in a narrow cone, which indicates AgNW is promising to be used for light-trapping. The proportion of light being ohmically absorbed in AgNW can reach about 13.1%, therefore, schemes to reduce the harm introduced by it must be taken into account in device design. Besides, the light capture abilities of AgNW, not only the maximum at RW but also the average values in waveband 0.2-0.6μm, are found to be approximately linear to the length; but RW is weakly length dependent. Such feature points out a simply way to manipulate the light capture ability of AgNW. Additionally, we also found that the light capture efficiency of AgNW arrives at the maximum under incidence paralleling to the nanowire. The insights obtained in this work provide useful guidelines for the design and optimization of devices using AgNW as the building block.

Funding

National High-tech Research and Development Program of China (863 Program, No. 2015AA034601); National Natural Science Foundation of China (Grant nos. 91333122, 51402106, 51372082, 61204064 and 51202067); Ph.D. Programs Foundation of Ministry of Education of China (Grant nos. 20130036110012); Par-Eu Scholars Program; Fundamental Research Funds for the Central Universities.